Corrosion of Ferritic Steels in High Temperature Molten Salt Coolants for Nuclear Applications

J. Farmer, B. El-Dasher, M. Serrano de Caro, J. Ferreira

December 1, 2008

Disclaimer

This document was prepared as an account of work sponsored by an agency of the United States government. Neither the United States government nor Lawrence Livermore National Security, LLC, nor any of their employees makes any warranty, expressed or implied, or assumes any legal liability or responsibility for the accuracy, completeness, or usefulness of any information, apparatus, product, or process disclosed, or represents that its use would not infringe privately owned rights. Reference herein to any specific commercial product, process, or service by trade name, trademark, manufacturer, or otherwise does not necessarily constitute or imply its endorsement, recommendation, or favoring by the United States government or Lawrence Livermore National Security, LLC. The views and opinions of authors expressed herein do not necessarily state or reflect those of the United States government or Lawrence Livermore National Security, LLC, and shall not be used for advertising or product endorsement purposes.

Corrosion of Ferritic Steels in
High Temperature Molten Salt Coolants for Nuclear Applications

Joseph Farmer[1], Bassem El-dasher[1], Magdalena Serrano de Caro[1], and James Ferreira[1]

[1]Lawrence Livermore National Laboratory, Livermore, CA 94550, USA

ABSTRACT

Corrosion of ferritic steels in high temperature molten fluoride salts may limit the life of advanced reactors, including some hybrid systems that are now under consideration. In some cases, the steel may be protected through galvanic coupling with other less noble materials with special neutronic properties such a beryllium. This paper reports the development of a model for predicting corrosion rates for various ferritic steels, with and without oxide dispersion strengthening, in FLiBe (Li_2BeF_4) and FLiNaK (Li-Na-K-F) coolants at temperatures up to 800°C. Mixed potential theory is used to account for the protection of steel by beryllium, Tafel kinetics are used to predict rates of dissolution as a function of temperature and potential, and the thinning of the mass-transfer boundary layer with increasing Reynolds number is accounted for with dimensionless correlations. The model also accounts for the deceleration of corrosion as the coolants become saturated with dissolved chromium and iron. This paper also reports electrochemical impedance spectroscopy of steels at their corrosion potentials in high-temperature molten salt environments, with the complex impedance spectra interpreted in terms of the interfacial charge transfer resistance and capacitance, as well as the electrolyte conductivity. Such in situ measurement techniques provide valuable insight into the degradation of materials under realistic conditions.

INTRODUCTION

Laser initiated fusion-fission (LIFE) engines have now been designed to produce nuclear power from natural or depleted uranium without isotopic enrichment, and from spent nuclear fuel from light water reactors without chemical separation into weapons-attractive actinide streams. A point-source of high-energy neutrons produced by laser-generated, thermonuclear fusion within a target is used to achieve ultra-deep burn-up of the fertile or fissile fuel in a sub-critical fission blanket. Fertile fuels including depleted uranium (DU), natural uranium (NatU), spent nuclear fuel (SNF), and thorium (Th) can be used. Fissile fuels such as low-enrichment uranium (LEU), excess weapons plutonium (WG-Pu), and excess highly-enriched uranium (HEU) may be used as well. Based upon preliminary analyses, it is believed that LIFE could help

meet worldwide electricity needs in a safe and sustainable manner, while drastically shrinking the nation's and world's stockpile of spent nuclear fuel and excess weapons materials. LIFE takes advantage of the significant advances in laser-based inertial confinement fusion that are taking place at the NIF at LLNL where it is expected that thermonuclear ignition will be achieved in the 2010-2011 timeframe.

The fusion-fission chamber is the heart of the LIFE Engine. Materials for fusion-fission hybrid reactors fall into several broad categories, including: (1) lasers and optics, (2) fusion targets, (3) tungsten first wall, (4) neutron multiplication blanket, (5) sub-critical fission blanket, (6) structural and cladding materials, (7) coolants and/or liquid fuels, (8) reflector, and (9) balance of plant. Issues related to lasers and optics, as well as fusion targets are discussed elsewhere. The LIFE engine's structural challenges include: need for high-temperature strength; resistance to high-temperature creep; immunity to radiation damage, including swelling and helium embrittlement; resistance to corrosion and environmental cracking in high-temperature molten fluoride salts; and the ability to be fabricated into necessary shapes and configurations with practical welding processes. It is hoped that the structural challenges can be met with oxide dispersion strengthened (ODS) ferritic steels [1-5]. This article focuses on the interaction of structural materials with coolants and/or liquid fuels.

Preferred coolants are FLiBe (Li_2BeF_4) in the primary coolant loop and FLiNaBe ($LiNaBeF_4$) in the secondary coolant loop [6-8]. Note that FLiBe is a binary mixture of lithium and beryllium fluorides ($2LiF + BeF_2 = Li_2BeF_4$). The FLiBe input temperature is 620°C and the exit temperature for this design is 680°C. The transmutation of lithium in these coolants produces tritium for the steady stream of fusion targets that must be fed to the LIFE engine, thereby making the system self sufficient in tritium. Unfortunately, this reaction also produces very corrosive hydrofluoric acid species (HF and TF), which can rapidly degrade structural and cladding materials. In the case of homogenous liquid fuels, UF_4 and ThF_4 can be dissolved in these molten salt mixtures.

CORROSION MECHANISMS & MODELS

The relative corrosion susceptibility of refractory metals and Fe-Cr steels can be understood by ranking the free energies of formation for their respective fluoride salts [9]. The transmutation of lithium in the Li_2BeF_4 forms corrosive tritium fluoride, which behaves chemically like hydrogen fluoride, or hydrofluoric acid. Published data indicate that the Cr_2O_3 film provides only limited corrosion protection. The preferential dissolution of chromium into the Li_2Be_4 salt results in the formation of a chromium depletion layer, which lies below a mixed oxide film of $Fe(Fe,Cr)_2O_4$ and disperse deposit of Fe_2O_3 particles [10]. While the presence of metallic beryllium has a positive effect on the formation of corrosive HF (TF), it promotes formation of problematic gaseous BeH_2. The postulated corrosion mechanisms for steels in molten fluoride salts are very complicated and are illustrated in Figure 1.
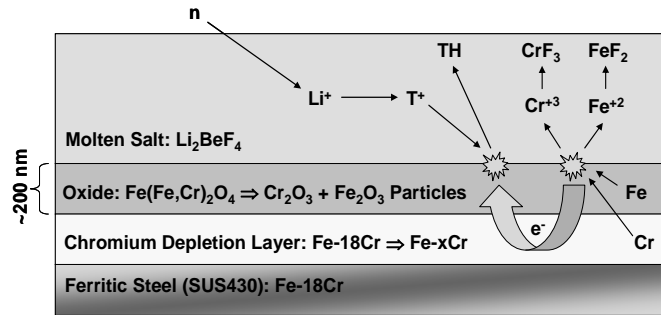
Figure 1. Corrosion mechanism for ODS ferritic steel in molten FLiBe based upon discussion in the literature.

Mixed potential theory

When two metals are galvanically coupled, a intermediate mixed potential is established. The exact position of this mixed potential, which is located between the oxidation-reduction potentials of the coupled metals, is determined by their relative electrode kinetics. The intersection of the anodic and cathodic Tafel lines identifies the formal mixed potential. This will be the rest potential of both galvanically coupled metals. At this potential, one metal will undergo anodic dissolution, while the other will be cathodically protected, with the possible recombination of hydrogen ions on the surface. By galvanically coupling either metallic lithium or beryllium to iron immersed in a blanket of FLiBe, a mixed potential will be established for the couple between the two reduction-oxidation (redox) potentials. As shown in Figure 2, mixed potential theory applied to ODS ferritic steel with sacrificial Be in molten Li_2BeF_4. In this case, the anodic Tafel line is assumed to be due to the anodic dissolution of sacrificial beryllium, as well as iron and chromium from the ODS, while the cathodic Tafel line is assumed to be due to the electrolytic reduction of tritium fluoride.

Corrosion rate limited by corrosion product solubility

Corrosive attack of ODS ferritic steel by Li_2BeF_4 and Li-Na-K-F coolants will probably be limited by saturation of the electrolyte with dissolved iron and chromium [8]. A simple model has been developed to account for the dissolution of LIFE Engine materials in the high temperature FLiBe and FLiNaK. This model assumes a constant rate of corrosion until the solution becomes saturated with chromium. If the molten salt coolant or fuel saturates with iron and chromium corrosion products, the continued dissolution of the ODS ferritic steel should cease. The case shown in Figure 3 assumes a constant rate of attack of 70.1 mils per year, and cessation of corrosion at the point where the salt becomes saturated with dissolved chromium at a concentration of 3000 ppm.
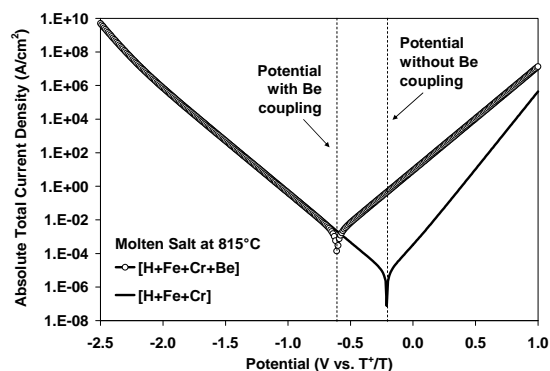
Figure 2. Mixed potential theory applied to ODS ferritic steel with and without sacrificial beryllium anode in molten Li$_2$BeF$_4$ at 815°C. This figure clearly shows the cathodic shift of the open circuit corrosion potential due to galvanic coupling of beryllium and ODS steel at 815°C.
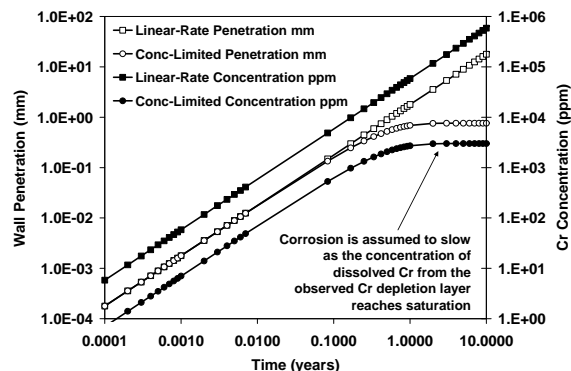

Figure 3. Limited corrosive attack of ODS by molten salts, assuming a rate of attack of 70.1 mils per year, and saturation of the salt with chromium at a concentration of approximately 3000 ppm.

EXPERIMENTAL

High temperature cell and scanning electron microscopy

An electrochemical cell developed by LLNL for corrosion testing of structural and cladding materials in high-temperature molten fluoride salts is shown in Figure 4a. The working electrode (larger disk of ODS steel on left), reference electrode (smaller disk of ODS steel on right), and counter electrode (platinum bar suspended above the two ODS steel disks) are shown in Figure 4b. The material being tested is held in the electrochemical by a machined ceramic plug. Figure 4c shows the cell being operated at 800°C. The corrosive attack of an early ODS steel sample, which is a powder metallurgy product, is shown in Figure 4d. The molten salt infiltrated the re-crystallized and damaged surface layer, which had a thickness of approximately 200 microns, and dissolved chromium oxide inclusions within the layer. Improved ODS steels are being developed to eliminate this problem.
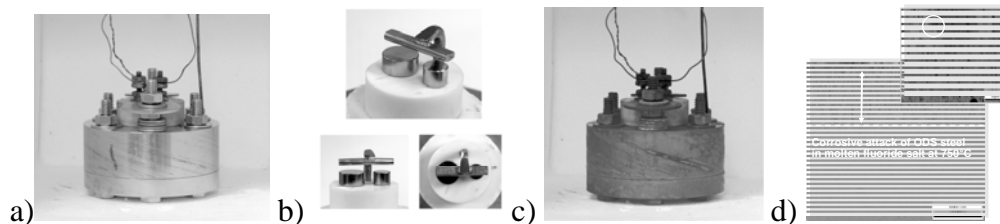

Figure 4 – Electrochemical cell for corrosion testing in high-temperature molten fluoride salts, with corrosion of working electrode shown

Electrochemical impedance spectroscopy

The three-electrode electrochemical cell shown in Figure 4a enable the corrosion of the ODS steel working electrode linear polarization and electrochemical impedance spectroscopy (EIS). The working electrode shown in Figure 4b was subjected to a small amplitude (± 5 mV) potential modulation centered at the open circuit corrosion potential, and the resultant current response measured. The modulation voltage and the current response are separated by a phase angle [11]. The electrical resistance of high-temperature electrochemical cell for testing structural and cladding materials in high-temperature molten-salt environments is shown in Figure 5a, with the melting of the salt and sample wetting as the cell evident as the cell was heated to 800°C. The ability to perform in situ electrochemical impedance spectroscopy (EIS) of steel surface in molten-salt at 800°C has been demonstrated, as shown in Figure 5b.

The most common equivalent circuit for an electrochemical cell includes the solution resistance, the charge-transfer resistance, the double-layer capacitance and the Warburg impedance associated with mass-transport limitations. Unfortunately, the behavior of a real system may not conform to a simple single-time constant Nyquist or Bode plot. Other effects due to evolving interfacial structure of the corroding sample, including the passive oxide film and the chromium depletion layer, must be captured with additional interfacial impedances to fully explain experimental observations. Additional time constants can be captured by sequentially combining parallel and series impedances until enough complexity has been included to account for observations. The reader is referred to more detailed publications for additional information on materials issues related to the LIFE project, including issues pertaining to corrosion [12,13].

a)   b)
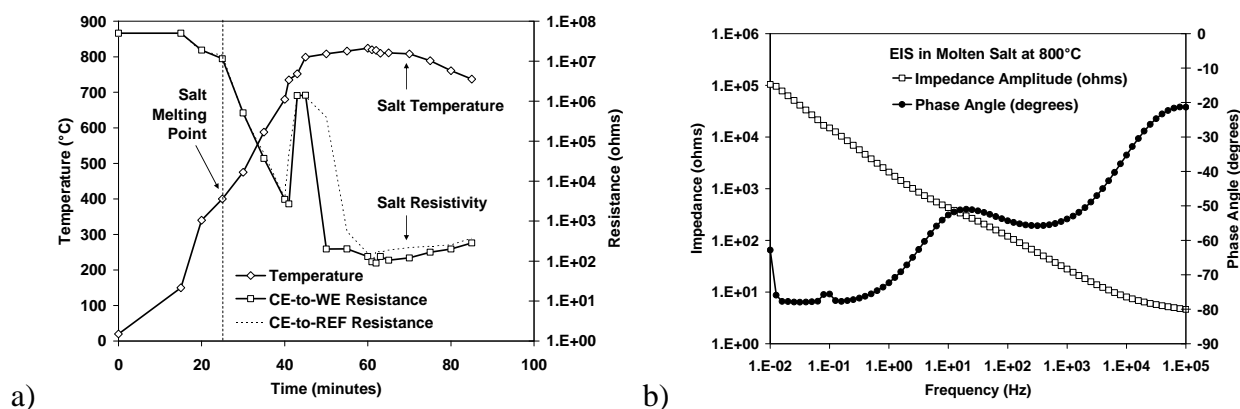
Figure 5. (a) Electrical resistance of high-temperature electrochemical cell for testing structural and cladding materials in high-temperature molten-salt environments showing the melting of the salt and wetting of the sample as the cell is heated to 800°C. (b) The ability to perform in situ electrochemical impedance spectroscopy (EIS) of steel surface in molten-salt at 800°C has been demonstrated.

SUMMARY

The corrosion of ODS ferritic steel in high-temperature molten-salt coolants is discussed. The application of mixed potential theory, which serves as the basis for predicting the open circuit corrosion potential, and for predicting the beneficial effects of sacrificial anodes, and a model for solubility limited rates of corrosion in molten salts are reviewed. EIS and SEM data at high temperature are also discussed

ACKNOWLEDGEMENTS

REFERENCES

1. T. R. Allen et al., Nucl. Sci. Eng. 151 (2005) 305–312.

2. S. Ukai et al., J. Nucl. Sci. Tech. 42, 1 (2005) 109-122.

3. R. L. Klueh et al., Nucl. Matls. 367-370 (2007) 48-53.

4. R. Schaublin et al., J. Nucl. Matls. 351 (2006) 247-260.

5. S. Ukai et al., J. Nucl. Matls. 307-311 (2002) 749-757.

6. D. A. Petti et al., Fusion Eng. Des. 81 (2006) 1439-1449.

7. I. N. Sviatoslavsky et al., Fusion Eng. Des. 72 (2004) 307-326.

8. D. F. Williams, ORNL/TM-2006/12, Oak Ridge National Laboratory, 2006.

9. E. T. Cheng et al. Fusion Eng. Des. Fusion Eng. Des. 69 (2003) 205-213.

10. H. Nishimura et al., Fusion Eng. Des. 58-59 (2001) 667-672.

11. A. J. Bard, L. R. Faulkner, Electrochemical Methods, Fundamentals and Applications, John Wiley & Sons, New York, NY, 1980, pp. 44-85; 86-135; 28-315; 316-369.

12. J. C. Farmer, LLNL-TR-407386 Rev. 1, Lawrence Livermore National Laboratory, 2008.

13. J. C. Farmer, LLNL-TR0408952 Rev. 0, Lawrence Livermore National Laboratory, 2008.